Journal of Solid State Chemistry **158,** 343–348 (2001)
doi:10.1006/jssc.2001.9123, available online at http://www.idealibrary.com on IDEAL®

Structural Evidence for Ferroelectricity in Eu_2GeS_4

Markus Tampier and Dirk Johrendt[1]

Institut für Anorganische Chemie und Strukturchemie II, Heinrich-Heine-Universität Düsseldorf, Universitätsstrasse 1, D-40225 Düsseldorf, Germany

Received November 1, 2000; in revised form January 17, 2001; accepted February 9, 2001

DEDICATED TO PROFESSOR WOLFGANG JEITSCHKO ON THE OCCASION OF HIS 65TH BIRTHDAY

A ferroelectric phase transition was detected in monoclinic europiumthiogermanate Eu_2GeS_4 ($T = 298$ K: $a = 6.639(1)$ Å, $b = 6.674(1)$ Å, $c = 8.146(1)$ Å, $\beta = 108.19(4)^\circ$, $Z = 2$) by means of temperature-dependent single-crystal X-ray structure determinations. At 298 K, the structure is polar with the space group $P2_1$ (α-Eu_2GeS_4), but above $T_C \approx 335$ K it is centrosymmetric with the space group $P2_1/m$ (β-Eu_2GeS_4). Main contributions to the transition are an antidistortive tilt of the thiogermanate tetrahedra and shifts of the europium ions, whose coordination numbers change from 7 to 6(+2). Small opposing displacements of europium and sulfur ions (0.09–0.11 Å) produce a permanent polarization parallel to the b axis. The phase transition corresponds to a condensing optical mode of A_u symmetry. From the analysis of thermal displacement parameters above T_C, it follows that the transition mechanism is partially displacive due to shifts of the europium sites and partially order–disorder due to the ordering of two sulfur atom sites. Below T_C, the evolution of the order parameters results in a critical exponent $\beta \approx \frac{1}{4}$, which is phenomenological interpreted within the Landau theory. Similarities and differences between the phase transitions of Eu_2GeS_4 and of isostructural halide ferroelectrics are discussed. From the structural viewpoint, Eu_2GeS_4 should be ferroelectric below $T_C \approx 335$ K and paraelectric above this temperature.

Key Words: **chalcogenide; thiogermanate; crystal structure; phase transition; ferroelectrics.**

INTRODUCTION

Ferroelectric materials exhibit a reorientable spontaneous polarization on cooling below a certain temperature, T_C, called the Curie point. Owing to their outstanding physical properties, ferroelectrics have received an enormous deal of attention in science (1–3) and technology (4,5). The biggest use of ferroelectric materials has been in the areas such as capacitor applications, thin films for nonvolatile memories, medical ultrasound imaging, and electrooptical data storage.

Up to now, solely metal oxide ferroelectrics are technically of significance, and therefore of course, these materials were most intensively studied. Beyond the oxides, ferroelectric chalcogenides are few and mainly confined to the SbSI and $Sn_2P_2S_6$ families (6,7). An important difference emerges from the fact that oxides are insulators, but chalcogenides are usually semiconductors with various bandgaps. Particularly the coexistence of light-induced free carriers and ferroelectricity results in new properties, summarized as photoferroelectric phenomena (8).

A promising chalcogenide compound is europiumthiogermanate, first reported in 1979 by Bugli *et al.* (9). Eu_2GeS_4 crystallizes in the space group $P2_1$ at room temperature. The structure is a variant of the Sr_2GeS_4 type (10), built up by almost undistorted $[GeS_4]^{4-}$ tetrahedra, separated and charge balanced by Eu^{2+} ions. This polar structure of Eu_2GeS_4 at room temperature is almost identical with the ferroelectric phase of K_2ZnBr_4, which transforms into its paraelectric form with the space group $P2_1/m$ at the Curie temperature $T_C = 155$ K (11, 12). This raises the question of whether Eu_2GeS_4 undergoes the same phase transition. In this case, it seems highly probable that this chalcogenide represents a new ferroelectric material.

So far, a $P2_1 \rightarrow P2_1/m$ transition of Eu_2GeS_4 was assumed to be unlikely (13). But this conclusion was drawn from the estimation of T_C by the AKJ relationship $T_C \approx K(\Delta y)^2$, where Δy is the largest atomic coordinate shift (14). However, it is easy to show that the AKJ relationship is unsuitable for predicting phase transitions in such systems. When T_C depends on Δy, it is important to determine the structure at temperatures well below the Curie point in order to ensure the transition is completed. Moreover, in the case of a continuos (second-order) transition, the displacement Δy itself depends on the temperature and consequently it cannot be set proportional to T_C. As an example, the AKJ relation predicted the T_C of K_2ZnBr_4 to be 151 K (15), in good agreement with the experimental value of 155 K. However, the coordinates were measured at 144 K, only

[1] To whom correspondence should be addressed. Fax: (+49)(0)211-8114146. E-Mail: johrendt@uni-duesseldorf.de.

0022-4596/01 $35.00

11 K below the second-order transition (16). When we use Δy values obtained from precise structural data measured by Bärnighausen at 128 K (17), we get a predicted T_C of 245 K, which is almost 100 K higher than the experimental value.

In the present paper, we report the structural evolution of Eu_2GeS_4 with respect to temperature in order to shed light on the question of whether europiumthiogermanate undergoes a ferroelectric phase transition and of which nature it would be.

EXPERIMENTAL SECTION

Sample Preparation and Characterization

Powder samples of Eu_2GeS_4 were synthesized from the elements (purity > 99.5%) in two steps. (i) The binary alloy Eu_2Ge was prepared by heating stochiometric mixtures of europium metal and germanium powder at 1123 K for 10 h in alumina crucibles, sealed in quartz glass ampoules under argon atmosphere. (ii) After homogenization in an argon-filled glove box, Eu_2Ge was oxidized with stochiometric amounts of sulfur at 1023 K for 15 h. The samples were homogenized again and reheated to 1023 K for 50 h. This procedure results in bright orange powders of Eu_2GeS_4, which are stable in air and insoluble in common organic solvents. X-ray powder patterns (HUBER G600, Cu$K\alpha_1$, silicon as external standard) detected no impurities and could be indexed with the monoclinic cell parameters taken from the literature (9).

Crystallographic Studies

Small irregular-shaped crystals (diameter ≈ 0.05 mm), suitable for X-ray experiments, were selected directly from the powder samples and carefully inspected by orienting Weissenberg photographs (Cu$K\alpha$). For the high-temperature measurements, the crystal was fixed in the narrow part of a quartz capillary (diameter 0.2 mm), which was evacuated, sealed under an argon atmosphere, and mounted on a NONIUS crystal heater goniometer head. This equipment allows crystal temperatures up to 500 K with an accuracy of $\pm$ 1 K. Temperatures below 295 K were realized by a standard flowing nitrogen apparatus. Lattice constants were determined between 298 and 378 K in steps of 5 or 10 K on a four-circle STOE STADI4 diffractometer (Mo$K\alpha_1$, graphite monochromator) using 39 strong reflections with $15^\circ \leq 2\theta \leq 35^\circ$. Each reflection was measured at the $\pm 2\theta$ position in order to correct crystal miscentering. The lattice parameters were refined by least squares methods to accuracies better then 10^{-3} Å.

Unique data sets ($3^\circ \leq 2\theta \leq 60^\circ$) were collected at $T = 185, 240, 285, 295, 310, 315, 320, 325, 330, 350, 380$, and 410 K. The STADI4 (18) software was used for data collection and X-RED (19) for data extraction and reduction. Absorption corrections were performed numerically using crystal shapes optimized by ψ-scan data using X-SHAPE (20). All least squares refinements with SHELXL-97 (21) converged to residuals $wR_2 = 0.04$–0.05 and $R_1 = 0.03$–0.04 for all F_o^2 data by using the atomic positions from Ref. (9) as initial parameters. Refinement cycles in the noncentrosymmetric space group $P2_1$ were performed with regard to twin domains convertible by inversion.

TABLE 1
Crystallographic Data and Details of the Data Collections for α- and β-Eu_2GeS_4

Formula		Eu_2GeS_4(9)[a]	α-Eu_2GeS_4	β-Eu_2GeS_4
Temperature		298 K	298 K	380 K
Wavelength (Å)		0.71073	0.71073	0.71073
Crystal system		Monoclinic	Monoclinic	Monoclinic
Space group		$P2_1$ (No. 4)	$P2_1$	$P2_1/m$ (No. 12)
a (Å)		6.638(1)	6.639(1)	6.643(2)
b (Å)		6.672(1)	6.674(1)	6.674(2)
c (Å)		8.146(1)	8.146(1)	8.162(2)
β (E)		108.20(2)	108.19(4)	108.19(4)
Volume (Å^3)		342.7(2)	342.9(2)	343.7(3)
Z		2	2	2
Density (g/cm^3)		4.89	4.889	4.878
μ (mm^{-1})		23.5	23.51	23.46
T_{min}, T_{max}		—	0.352, 0.858	0.352, 0.858
Flack parameter		—	0.297(6)	—
Diffractometer		CAD-4, Nonius	AED-2, Stoe	AED-2, Stoe
2θ range		$2^\circ \leq 2\theta \leq 70^\circ$	$2^\circ \leq 2\theta \leq 60^\circ$	$2^\circ \leq 2\theta \leq 60^\circ$
Independent refl.		1214	2033	1097
R_1/wR_2		0.032/—	0.032/0.041	0.041/0.048
Atomic coordinates[b]				
Eu1	x	0.7184(1)	0.7185(1)	0.7182(1)
	y	0.2343 (Fixed)	0.2371(4)	$\frac{1}{4}$
	z	0.0521(1)	0.0521(1)	0.0516(1)
Eu2	x	0.7673(1)	0.7674(1)	0.7681(1)
	y	0.2321(5)	0.2355(4)	$\frac{1}{4}$
	z	0.5678(1)	0.5678(1)	0.5681(1)
Ge	x	0.2731(2)	0.2734(1)	0.2738(1)
	y	0.2500(6)	0.25 (Fixed)	$-\frac{1}{4}$
	z	0.2001(2)	0.2006(1)	0.2008(1)
S1	x	0.0968(7)	0.0975(4)	0.0996(4)
	y	0.2732(9)	0.2671(9)	$\frac{1}{4}$
	z	−0.0767(5)	−0.0765(3)	−0.0755(3)
S2	x	0.0783(6)	0.0785(4)	0.0789(4)
	y	0.264(1)	0.2613(9)	$\frac{1}{4}$
	z	0.3738(5)	0.3731(3)	0.3734(2)
S3	x	0.485(1)	0.4866(9)	0.4949(2)
	y	−0.010(1)	−0.0105(8)	−0.0039(2)
	z	0.257(1)	0.2589(9)	0.2610(2)
S4/3′	x	0.505(1)	0.5031(8)	[0.4949(2)]
	y	0.4971(9)	0.4973(8)	[0.4961(2)]
	z	0.264(1)	0.2628(9)	[0.2610(2)]

[a] The *cba* setting of the unit cell given in (9) is transformed to the standard *abc* setting.

[b] Numbers in round brackets are the standard deviations of the last significant digit; coordinates in square brackets are the symmetry equivalent positions of S3 in $P2_1/m$, S3′.

TABLE 2
Anisotropic Displacement Parameters (pm^2) for α-Eu_2GeS_4 (298 K) and β-Eu_2GeS_4 (380 K)

	U_{11}		U_{22}		U_{33}		U_{23}		U_{13}		U_{12}	
	α	β	α	β	α	β	α	β	α	β	α	β
Eu1	147(2)	207(2)	234(3)	340(3)	116(2)	160(2)	− 2(1)	0	66(1)	92(2)	− 4(5)	0
Eu2	165(2)	228(2)	249(3)	350(3)	124(3)	171(2)	14(5)	0	79(1)	109(2)	− 7(5)	0
Ge	119(4)	158(4)	108(5)	153(4)	124(3)	168(4)	3(8)	0	69(3)	89(3)	8(8)	0
S1	191(10)	272(11)	401(27)	599(17)	113(9)	145(9)	6(14)	0	54(7)	79(8)	− 38(14)	0
S2	151(9)	230(10)	385(25)	580(17)	142(9)	177(9)	− 36(16)	0	96(7)	133(8)	− 23(15)	0
S3	197(23)	232(6)	91(17)	150(6)	186(27)	232(6)	− 3(13)	3(5)	99(19)	106(6)	19(13)	24(5)
S4	136(21)		125(18)		148(25)		2(14)		57(16)		− 13(13)	

RESULTS AND DISCUSSION

The first structure determination of Eu_2GeS_4 was performed at 298 K. Refinements of the atomic parameters confirmed the structure in the space group $P2_1$ as given in the literature within the standard deviations. Crystallographic data, final coordinates, and anisotropic displacement parameters are summarized in the Tables 1 and 2; selected interatomic distances and bond angles are compiled in Table 3.

The crystal structure of Eu_2GeS_4 at room temperature is depicted in Fig. 1. Europium is seven-coordinated; six sulfur atoms form a trigonal prism and one additional sulfur is located over one rectangular plane. Due to small shifts in y, the Eu–S distances along the b axis alternate between 3.35 and 3.75 Å, as emphasized by solid and dashed bonds in Fig. 1. Since positive and negative charged atoms are shifted by ~ 0.09–0.11 Å in opposite directions along the polar axis, the compound should have a permanent polarization parallel to b.

In order to detect a possible phase transition, we have determined the lattice constants of a single crystal between 298 and 378 K on the four-circle diffractometer. As seen from the diagrams shown in Fig. 2, the slopes of $a(T)$ and $c(T)$ changes at $T \approx 335$ K, whereas $b(T)$ runs through a significant minimum at this temperature. The monoclinic angle remained constant within the error and is therefore not shown here. Due to the changes in the courses of the lattice constants, the resulting unit cell volumes show the same anomaly. All parameters vary continuously within the experimental resolution of 10^{-3} Å, which hints that the transition to had at least a strong second-order component. This evolution of the lattice parameters is similar to that of ferroelectric K_2ZnBr_4 (17) but not identical, because the transition temperature of Eu_2GeS_4 is much higher and the halide shows no minimum in $b(T)$. The latter effect was

TABLE 3
Selected Interatomic Distances[a] (Å) and Bond Angles (E) for α-Eu2GeS4 (298 K) and β-Eu_2GeS_4 (380 K)

	α-Eu_2GeS_4	β-Eu_2GeS_4		α-Eu_2GeS_4	β-Eu_2GeS_4
Eu1–S2	2.945(3)	2.951(3)	Eu2–S2	2.976(2)	2.973(2)
–S3	2.993(6)	2.993(2) 2×	–S4/3′	3.034(6)	3.036(2) 2×
–S4/3′	2.991(6)		–S3	3.033(6)	
–S1	3.018(3)	3.022(3)	–S1	3.046(3)	3.052(3)
–S3	3.092(6)	3.094(2) 2×	–S4/3′	3.096(6)	3.099(2) 2×
–S4/3′	3.089(6)		–S3	3.094(6)	
–S1	3.350(5)	3.533(1) 2×	–S2	3.314(6)	3.477(2) 2×
–S1	3.727(5)		S2	3.645(6)	
Ge–S1	2.196(3)	2.190(2)	S3–Ge–S4/3′	101.0(1)	101.0(1)
–S2	2.189(2)	2.191(2)	S1–Ge–S2	115.3(1)	115.7(1)
–S3	2.198(6)	2.195(2) 2×	S1–Ge–S4/3′	107.9(2)	109.4(1) 2×
–S4/3′	2.196(6)		S1–Ge–S3	111.3(2)	
			S2–Ge–S3	111.0(3)	110.2(1) 2×
			S2–Ge–S4/3′	109.4(2)	

[a] S3′ means the symmetry equivalent position of S3 in $P2_1/m$.

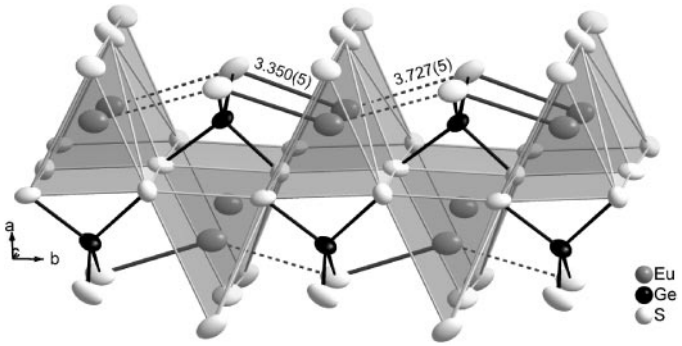

FIG. 1. Crystal structure of α-Eu_2GeS_4 at 298 K (thermal ellipsoids at 95% probability).

observed in the well-known ferroelectric triglycine sulfate (TGS) (2). In the following, we denote the modification below 335 K as α-Eu_2GeS_4 and the form stable above the transition temperature as β-Eu_2GeS_4.

The structure of the high-temperature modification β-Eu_2GeS_4 was obtained from single crystal data, collected at 380 K. Subsequent refinements of the atomic positions in the space group $P2_1$ converged now at $y = \frac{1}{4}$ for the atoms Eu1, Eu2, S1, and S2 within the standard deviations. From this it is clear that β-Eu_2GeS_4 has the space group symmetry $P2_1/m$, where these atoms are located on mirror planes at $y = \frac{1}{4}$ and $\frac{3}{4}$. Thus, the structural phase transition is accompanied by a symmetry change from $P2_1$ to $P2_1/m$. Crystallographic data and the final parameters for β-Eu_2GeS_4 are summarized in the Tables 1 and 2. Important bond lengths and angles are given in Table 3, each in comparison with the data for α-Eu_2GeS_4. As seen from the crystal structure shown in Fig. 3, the coordination number of the Eu atoms has changed from 7 to 6(+ 2), because the Eu–S distances along b are equal now (dashed bonds in Fig. 3). Consequently, the permanent polarization vanishes and the paraelectric structure is formed.

The refinement cycles with the space group $P2_1/m$ resulted large anisotropic displacement parameters U_{22} (see the thermal ellipsoids in Fig. 3) for the atoms on the mirror planes at $y = \frac{1}{4}$, which indicate positional disorder. Static displacements are distinguishable from thermal motions by the temperature dependence of the mean square displacements (MSD), obtained from the diagonalized U_{ij} matrix. Figure 4 shows the MSD of Eu_2GeS_4 plotted against the absolute temperature. The striking larger values in both diagrams correspond to displacements of Eu1, Eu2, S1, and S2 perpendicular to the mirror plane in $P2_1/m$. Extrapolations to absolute zero for S1 and S2 gives static displacements of $\approx 200 \pm 50\,\mathrm{pm}^2$ or $\approx 0.14 \pm 0.03$ Å, in good agreement with the atomic shifts along b in the polar α-phase (see Table 1). In contrast to this, the extrapolations for the Eu atoms are almost zero at $T = 0$ within the error of

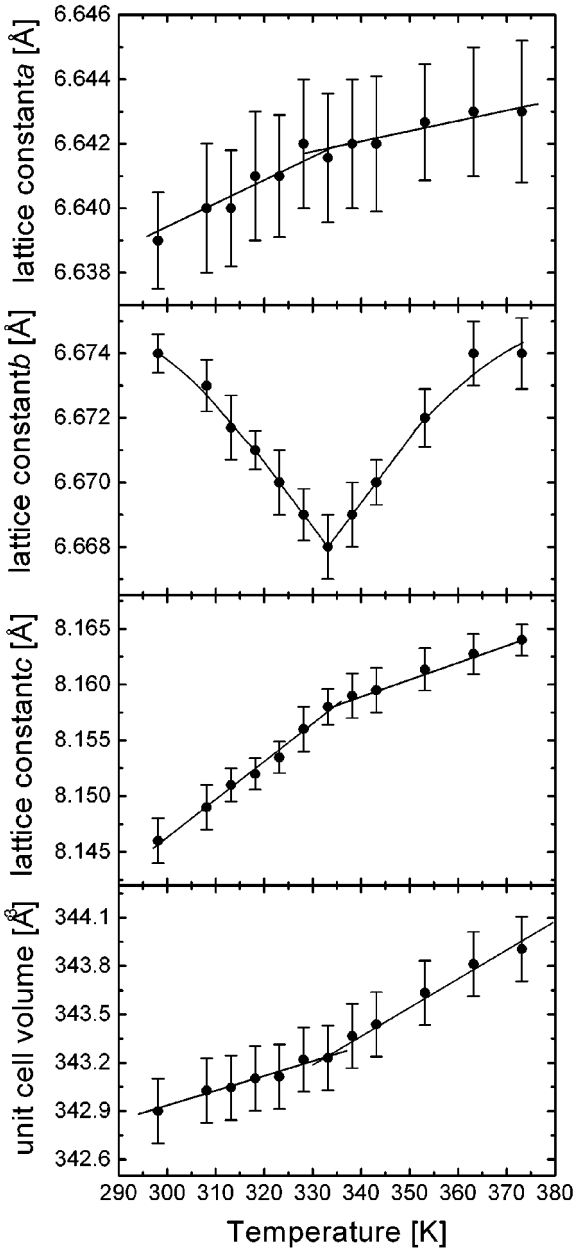

FIG. 2. Single-crystal lattice parameters and unit cell volumes of Eu_2GeS_4 against the temperature.

$\pm 50\,\mathrm{pm}^2$. Thus, the higher displacement parameters of the Eu atoms originate from enhanced thermal motion, whereas the S1 and S2 atoms are statically disordered. From this we can infer the complex mechanism of the of $P2_1 \rightarrow P2_1/m$ phase transition in Eu_2GeS_4 as proposed for K_2ZnBr_4. The transition is partially *displacive* regarding to small shifts of the Eu atoms ($y = \frac{1}{4} \rightarrow y = 0.243$) and partially *order–disorder* regarding the ordering of the S1 and S2 atoms.

The atomic coordinates of the displaced atoms transform according to the irreducible representation A_u of the point

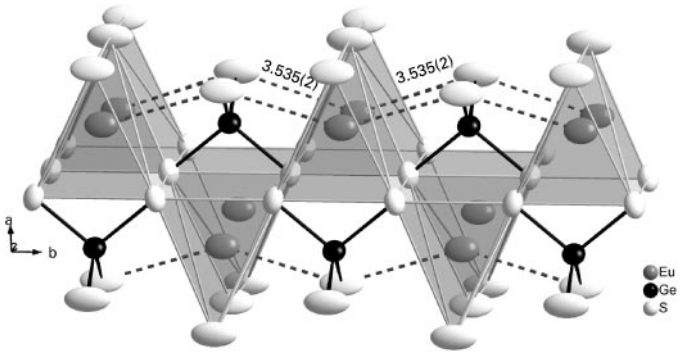

FIG. 3. Crystal structure of β-Eu_2GeS_4 at 380 K (thermal ellipsoids of 95% probability).

group C_{2h}. The phase transition is the condensation of an optical A_u-phonon branch as the temperature approaches T_C. This may be described from a chemical viewpoint in the following way. A "soft" mode emerges when the net restoring force opposing a lattice distortion vanishes. In the present case, the phonon causes periodic changes of the Eu1–S1 and Eu2–S2 distances in β-Eu_2GeS_4 (dashed bonds in Fig. 3). But the gain of bonding energy if one bond becomes shorter (3.53 Å → 3.35 Å) is larger than the energy loss due to the elongation of the other one (3.53 Å → 3.75 Å). As the temperature decreases, the restoring force cannot overcome this excess of bonding energy and the frequency drops to zero at T_C. The polarization vectors of this zero frequency normal mode describe precisely the observed lattice distortion.

During the phase transition, the shape of the GeS_4 tetrahedra and the position of the germanium atoms remain almost unchanged. Main contributions of the structural changes may be ascribed by cooperative tilts of the GeS_4-tetrahedra with a tilt axis [001]. The tilt angle η, evaluated form the atomic coordinates (17), has the right symmetry (A_u) to serve as an order parameter for the phase transition. This is also valid for the polarization vector P_S. Up to now, P_S could not be measured directly, since sufficiently large single crystals of Eu_2GeS_4 are not yet available; experiments to grow larger crystals are actually in progress. An ionic point charge model allows to approximate P_S form the atomic positions y_i, obtained by the X-ray structure determinations:

$$P_S = \frac{2b}{V} \sum_{i=1}^{7} q_i (y_i - y_{Ge}).$$

By taking the ionic charges $q = +2e$ for Eu and $q = -1e$ for S in $[GeS_4]^{4-}$, the lattice parameter b and the unit cell volume V determined at 298 K, we get $P_S = 4.9\ \mu C\,cm^{-2}$. If the atomic shifts may be regarded as one-dimensional, this ionic model should tend to give values of P_S smaller than those acquired via experiment, indicating the importance of a neglected electronic contribution (3).

The temperature dependencies of the order parameters P_S and η were deduced from subsequent structure determinations of α-Eu_2GeS_4 at various temperatures below T_C. As seen from Fig. 5, the order parameters (OP) show the typical behavior of a second-order phase transition. The solid and dashed lines represent fits to the power law $OP = a(T_C - T)^{\beta}$ and yields a critical exponent $\beta = 0.26 \pm 0.03 \approx \frac{1}{4}$. This value clearly supports a complex transition mechanism as proposed above, because the

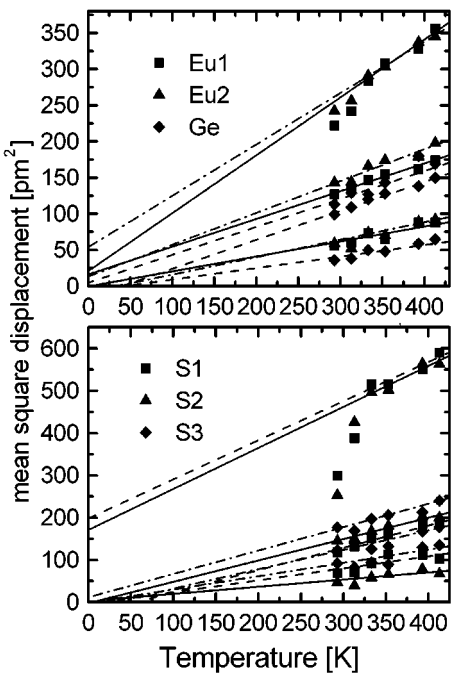

FIG. 4. Mean square displacements (MSDs) of Eu_2GeS_4 against the temperature and their extrapolations to absolute zero.

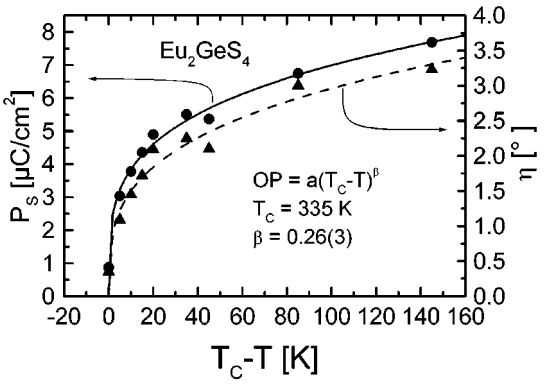

FIG. 5. Temperature dependence of the order parameters P_S and η in Eu_2GeS_4.

fourth-order term in the Landau free energy density, $\hat{F}$, may be neglected now against the sixth-order one (22):

$$\hat{F}(P,E) = -EP + g_0 + \tfrac{1}{2}g_2P^2 + \tfrac{1}{4}g_4P^4 + \tfrac{1}{6}g_6P^6 + \ldots$$

The coefficients g_i are temperature-dependent, and the equilibrium polarization is

$$\frac{\partial \hat{F}}{\partial P} = 0 = -E + g_2P + g_6P^5.$$

In order to get a polarized state ($P \neq 0$), the coefficient g_2 must vanish at a certain temperature T_0, i.e., $g_2 = \gamma(T - T_0)$, and the temperature dependency of the polarization P in zero external field ($E = 0$) gets

$$|P| = \left(\frac{\gamma}{g}\right)^{\frac{1}{4}}(T_0 - T)^{\frac{1}{4}}.$$

Although the critical exponent $\beta \approx \frac{1}{4}$ for the transition of Eu_2GeS_4 is not very precise due to the rather small number of data points, it agrees well with the theoretical model. This result proves again the similarity of the transitions of Eu_2GeS_4 and K_2ZnBr_4 ($\beta = 0.27 \pm 0.02$) (11).

By taking all structural features of the phase transition into account, we can draw the conclusion that Eu_2GeS_4 should be ferroelectric below $T_C = 335\,K$ and paraelectric above this temperature. Important differences to the isostructural ferroelectric halides (23) are as follows: (i) a much higher Curie temperature, (ii) a presumably higher polarization P_S, (iii) the minimum in the lattice constant b at T_C, (iv) the stability against air and moisture, and (v) the higher electrical conductivity of the chalcogenide. Preliminary measurements resulted in electrical resistivities in the order of magnitude of $1.5 \times 10^7\,\Omega cm$ at 298 K. However, dielectric measurements of single-crystal Eu_2GeS_4 are absolutely required in order to establish the ferroelectric properties definitely.

To our knowledge, Eu_2GeS_4 is the first chalcogenide that shows this type of ferroelectric transition. We have detected the same phenomenon for the isostructural compound Eu_2GeSe_4 with an even higher T_C of 620 K and $P_S \approx 7\,\mu C\,cm^{-2}$ at 298 K, whereas the $P2_1/m \rightarrow P2_1$ structural transition occurs in Ba_2SnSe_4 at 120 K with small atomic displacements. Details about these transitions will be reported in forthcoming papers.

ACKNOWLEDGMENTS

The authors are indebted to Prof. Dr. A. Mewis and Prof. Dr. W. Frank for their interest and financial support. D. J. thanks Prof. Dr. H. Bärnighausen for fruitful discussions and valuable help. This work was supported financially by the Deutsche Forschungsgemeinschaft (Jo257/3) and the Fonds der Chemischen Industrie.

REFERENCES

1. H. D. Megaw, "Ferroelectricity in Crystals." Methuen, London, 1957.
2. T. Mitsui, I. Tatsuzaki, and E. Nakamura, "An Introduction to the Physics of Ferroelectrics." Gordon and Breach, London, 1976.
3. M. E. Lines and A. M. Glass, "Principles and Applications of Ferroelectrics and Related Materials." Clarendon, Oxford, 1977.
4. J. M. Herbert, "Ferroelectric Transducers and Sensors." Gordon and Breach, London, 1982.
5. Y. Xu, "Ferroelectric Materials and Their Applications." North Holland, Amsterdam, 1991.
6. Landolt-Börnstein, "Ferroelectrics and Related Substances. Non-Oxides." Springer-Verlag, Berlin, 1990.
7. Y. Vysochanskii, *Ferroelectrics* **218**(1–4), 629 (1998).
8. V. M. Fridkin, "Ferroelectric Semiconductors." Consultants Bureau, New York, London, 1980.
9. G. Bugli, J. Dugué, and S. Barnier, *Acta Crystallogr.* **35B,** 2690 (1979).
10. E. Phillipot, M. Ribes, and M. Maurin, *Rev. Chim. Miner.* **8,** 99 (1971).
11. F. Shimizu, T. Yamaguchi, H. Suzuki, M. Takashige, and S. Sawada, *J. Phys. Soc. Jpn.* **59,** 1936 (1990).
12. M. Jochum, H.-G. Unruh, and H. Bärnighausen, *J. Phys. Condens. Matter* **6,** 5751 (1994).
13. J. Fábry, *Phase Transitions* **53,** 61 **(**1995).
14. S. C. Abrahams, S. K. Kurtz, and P. B. Jamieson, *Phys. Rev.* **172,** 551 (1968).
15. S. C. Abrahams, *Acta Crystallogr. B* **50,** 257 (1994).
16. J. Fábry, T. Breczewski, F. J. Zúñiga, and A. R. Arnaiz, *Acta Crystallogr. C* **49,** 946 (1993).
17. H. Bärnighausen, "IVth European Conference on Solid State Chemistry at Dresden (Germany) 1992," Book of Abstracts, S. 296.
18. STADI4 1.07. STOE & Cie GmbH, Darmstadt, 1995–1997.
19. X-RED 1.09, "Data Reduction Program." STOE & Cie GmbH, Darmstadt, 1997.
20. X-SHAPE 1.01, "Crystal Optimization for Numerical Absorption Correction." STOE & Cie GmbH, Darmstadt, 1996.
21. G. M. Sheldrick, "Shelxl-97 Program for Crystal Structure Refinement." Universität Göttingen, 1997.
22. C. Kittel, "Introduction to Solid State Physics," 4th ed. Wiley, New York, 1971.
23. S. Sawada, M. Takshige, F. Shimizu, H. Suzuki, and T. Yamaguchi, *Ferroelectrics* **169,** 207 (1995).